



# Influence of noble metals (Pd, Pt) on the performance of Ru/Al<sub>2</sub>O<sub>3</sub> based catalysts for toluene hydrogenation in liquid phase



Raphael Soeiro Suppino <sup>a,\*</sup>, Richard Landers <sup>b</sup>, Antonio José Gomez Cobo <sup>a</sup>

<sup>a</sup> Laboratory for Development of Catalytic Processes, Department of Chemical Systems Engineering, School of Chemical Engineering, University of Campinas, Cidade Universitária Zeferino Vaz, CEP 13083-852, Campinas, SP, Brazil

<sup>b</sup> Laboratory of Surface Physics, Department of Applied Physics, "Gleb Wataghin" Institute of Physics, University of Campinas, CEP 13083-859, Campinas, SP, Brazil

## ARTICLE INFO

### Article history:

Received 6 April 2016

Received in revised form 10 June 2016

Accepted 30 June 2016

Available online 1 July 2016

### Keywords:

Noble metal

Alumina

Catalyst activation

Formaldehyde

Toluene hydrogenation

## ABSTRACT

Catalytic hydrogenation of aromatic compounds is of great interest due to environmental aspects and the wide range of industrial processes involving such reaction. In this context, the present work aims to study the influence of Pd or Pt addition on the performance of Ru/Al<sub>2</sub>O<sub>3</sub> based catalysts for toluene hydrogenation in liquid phase. For this, catalysts were prepared by wet impregnation from chlorinated precursors and reduced in liquid phase by formaldehyde (H<sub>2</sub>CO). After impregnation, a part of the catalysts were activated ex situ at 573 K or in situ at 523 K under H<sub>2</sub>. The studied solids were characterized by N<sub>2</sub> physisorption, SEM + EDX, TEM, XPS and TPR techniques. Catalytic tests were conducted in a slurry Parr reactor at 373 K under constant H<sub>2</sub> pressure of 5 MPa. Results show that solids reduction by H<sub>2</sub>CO led to metallic species, while the activation treatments form oxides and decrease the catalytic activity. The initial reaction rate of non-activated monometallic catalysts follows the order: Ru/Al<sub>2</sub>O<sub>3</sub> ≫ Pd/Al<sub>2</sub>O<sub>3</sub> ≈ Pt/Al<sub>2</sub>O<sub>3</sub>. A synergistic effect on the activity of Ru/Al<sub>2</sub>O<sub>3</sub> based catalysts is induced by the Pt addition.

© 2016 Elsevier B.V. All rights reserved.

## 1. Introduction

Catalytic hydrogenation of aromatic compounds is of great interest due to environmental aspects and the wide range of industrial processes involving these reactions. It is an important route to obtain several chemical intermediates as well as to eliminate toxic aromatic compounds present in fuels [1,2]. Indeed, the hydrodearomatization is one of the most important processes in a petroleum refinery [3], having great influence on the final quality of diesel [4,5].

Most of the work found in the specialized literature focuses on the hydrogenation of benzene, notably aiming to obtain the partially hydrogenated product, cyclohexene [6–11]. In a recent paper, Foppa and Dupont [12] presented a thorough review regarding the main advances achieved for the partial hydrogenation of benzene in the last four decades.

However, recent efforts have been made to reduce the use of benzene in researches, since this compound is known to be highly carcinogenic. Hence, toluene has been employed as a substitute of

benzene due to its chemical similarities and lower toxicity [13–15]. In addition, the toluene hydrogenation is often used as probe reaction to test the performance of metal catalysts since it is considered insensitive with respect to surface structures [16].

Many catalysts have been tested on the hydrogenation of aromatics, amongst which noble metals such as Pd, Pt and Ru, usually supported on Al<sub>2</sub>O<sub>3</sub>, have shown higher activities and stability [3,13]. It is noteworthy that Ru based catalysts have been increasingly employed, since higher yields of the intermediate product are obtained in presence of this metal [11,17–19].

Although the incipient impregnation is a common method to prepare supported catalysts [12,20], the wet impregnation has been acknowledged as a method that leads to solids with higher metallic dispersion and consequently higher activity [8,11,21–23]. The characteristics of the solids prepared by wet impregnation may be affected by variables present in this method [24], such as the suspension temperature and pH. However, the reducing procedure appears to induce effects that are more important since it involves the formation of the active phase of these solids [23].

In wet impregnation, the catalyst reduction procedure is usually carried out in liquid-phase employing reducing agents such as sodium borohydride (NaBH<sub>4</sub>) [25], hydrazine (N<sub>2</sub>H<sub>4</sub>) [24] or formaldehyde (H<sub>2</sub>CO) [11], under mild conditions. However, high

\* Corresponding author.

E-mail addresses: [rsuppino@feq.unicamp.br](mailto:rsuppino@feq.unicamp.br), [raphaelsuppino@gmail.com](mailto:raphaelsuppino@gmail.com) (R.S. Suppino).

temperature reduction may also be conducted ex situ under H<sub>2</sub> flow [8,26,27].

Suppino et al. [11] studied the influence of the reduction method on the performance of Ru/Al<sub>2</sub>O<sub>3</sub> catalysts prepared by wet impregnation for partial hydrogenation of benzene in liquid phase. Catalyst reduction by H<sub>2</sub>CO led to a higher activity and selectivity of cyclohexene than the reduction ex situ under H<sub>2</sub> flow.

Groppi et al. [28] prepared Pd/Al<sub>2</sub>O<sub>3</sub> catalysts by wet impregnation using the following reducing agents: sodium formate (HCO<sub>2</sub>Na), NaBH<sub>4</sub> and H<sub>2</sub>. According to the authors, the reducing agents decrease the metal dispersion, which was related to a possible sintering of the Pd. The occurrence of Pd sintering was also suggested by other authors [29,30], according to whom the metallic particles may experience some degree of mobility even in relatively low temperatures, especially when the catalyst reduction is carried out under H<sub>2</sub> atmosphere.

The use of bimetallic catalysts for hydrogenation reactions has been subject of many studies. Bimetallic catalysts often present superior properties than the respective monometallic solids, such as higher tolerance against sulfur poisoning and thermal stability [19,31–34].

Romanenko et al. [31] studied the addition of Ru to Pd/C catalysts in order to prevent the Pd sintering by the solid reduction under H<sub>2</sub> flow. According to the authors, the Ru addition led to an increase of the metallic dispersion on the catalyst. Moreover, the bimetallic Pd-Ru/C catalyst has proven to be more resistant to sintering. Such effect was related to the increase of the potential energy barrier for the mobility of Pd species promoted by the presence of Ru.

More recently, Chen et al. [35] evaluated the effects of the addition of Pd to Ru based catalysts prepared by the wet co-impregnation method and reduced by NaBH<sub>4</sub>. According to the authors, bimetallic Ru-Pd catalysts presented superior catalytic activity over monometallic ones as well as smaller nanoparticle size with narrower distribution.

In this context, the present work aims to study the influence of Pd or Pt addition on the performance of Ru/Al<sub>2</sub>O<sub>3</sub> based catalysts for toluene hydrogenation in liquid phase.

## 2. Experimental

### 2.1. Catalysts preparations

Alumina (Al<sub>2</sub>O<sub>3</sub>) of commercial grade was used as received as catalysts support. According to the manufacturer (Alfa Aesar), the solid (99.9 wt%) is in the gamma phase, with an average particle diameter of 40 μm.

Mono and bimetallic catalysts were prepared from the precursors RuCl<sub>3</sub>·xH<sub>2</sub>O, PdCl<sub>2</sub> (Aldrich Chemical Co.) and PtCl<sub>2</sub> (Santa Cruz Biotechnology), all with 99.9 wt% of purity, in order to obtain a total metal mass fraction of 5 wt%.

Wet impregnation was used for the preparation of monometallic catalysts. In the procedure, deionized water was added to the support resulting in a suspension continuously agitated by a magnetic stirrer at room temperature.

Since both the Pd and Pt chlorides are insoluble in water, the precursors of such metals were previously dissolved in aqua regia (1 HCl:1 HNO<sub>3</sub>). The resultant solution was then heated under constant stirring until its complete vaporization, thus remaining a metal salt of Pd or Pt that was dissolved in water.

The aqueous solution of the metal (Pd, Pt or Ru) was then slowly added to the support suspension. Afterwards, the resultant suspension was heated until 353 K and then its pH was adjusted to 10 by adding a 2 M aqueous solution of NaOH.

In sequence, an aqueous solution of formaldehyde (H<sub>2</sub>CO, Merck, 37 wt%), used as reducing agent, was added to the sus-

pension. After this reduction in liquid phase, the suspension was filtered in a Büchner funnel and the remaining solid was thoroughly washed with deionized water in order to remove residual chlorine, sodium and formaldehyde. During the washing procedure, the chlorine and sodium eliminations were respectively observed by AgNO<sub>3</sub> and flame tests.

Afterwards, the solids were dried in an oven at 358 K for 24 h. After drying, a part of the obtained catalysts were submitted to ex situ or in situ activation. In the ex situ activation, the catalyst was placed in a Pyrex glass cell and heated at 10 K/min under H<sub>2</sub> flow of 40 mL/min from the room temperature until 573 K, remaining at this temperature for 3 h. Catalysts submitted to ex situ activation have the E abbreviation on its denominations.

In situ activation took place in the reactor itself, where the catalyst reduced by H<sub>2</sub>CO was submitted to the H<sub>2</sub> pressure of 3 MPa at 523 K during 1 h. Catalysts submitted to in situ activation have the I abbreviation on its denominations.

Bimetallic catalysts were prepared by co-impregnation, employing the wet impregnation procedure described above. It is noteworthy that only the ex situ activation was studied for bimetallic catalysts because of the little effect induced by in situ activation on the active phase formation of monometallic solids, as discussed hereafter.

### 2.2. Support and catalysts characterization

The support γ-Al<sub>2</sub>O<sub>3</sub> was characterized by potentiometric titration in order to determine its isoelectric point, an important parameter for the wet impregnation procedure. A digital micro-processed pH meter (Marconi, model MA522) was used to take pH measurements according to the procedure of Strelko and Malik [36].

The specific surface area (Sg) of the solids was determined through N<sub>2</sub> physisorption (B.E.T. method). A sample of 1.00 g of each solid was previously dried at 473 K under vacuum and the physisorption was conducted at 77 K in a Tristar Micromeritics ASAP 2010 equipment.

Scanning Electronic Microscopy (SEM) coupled with spectrometric X-ray analysis (SEM+EDX) was used mainly with the purpose of evaluating the chemical composition of the catalysts. The analyses were conducted in a LEO 440i Leica equipment. Before insertion in the SEM, all samples were covered with a fine layer of gold atoms using a 3 mA current for 180 s in order to obtain a gold film thickness of 92 Å.

Transmission Electronic Microscopy (TEM) analyses were carried out on a Libra 120 Zeiss microscope with Cantega 2k/Olympus CCD camera and iTEM data acquisition platform. The samples were gently grinded and then dispersed in water. The dispersion was placed on ultrasound for 10 min and then left to rest for another 10 min. A drop of the solution was placed on a 300 mesh copper grid coated with palladium and carbon. The grids were dried at ambient temperature and examined at 80 kV using the energy filter at zero loss, 25 eV, 30 eV or 50 eV. The energy positions of 25 eV and 50 eV correspond to the first and second plasmon.

X-ray Photoelectrons Spectroscopy (XPS) was employed in order to study the chemical compounds on the catalysts surfaces. A spherical analyzer VSWHA-100 with aluminum anode (AlK<sub>α</sub>, h<sub>v</sub> = 1486.6 eV) was used. The pressure during the analyses was lower than 2.10<sup>-12</sup> MPa. To correct binding energies, the line Al 2p with binding energy of 74.0 eV was used as reference.

The formation of the catalysts active phases was studied through temperature programmed reduction (TPR). A Micromeritics Auto Chem 2910 equipment was used to obtain the TPR profiles. In these analyses, a sample of 50 mg of each solid was heated at 10 K/min from 298 to 573 K under 50 mL/min flow of a 10% H<sub>2</sub> in N<sub>2</sub> mixture.

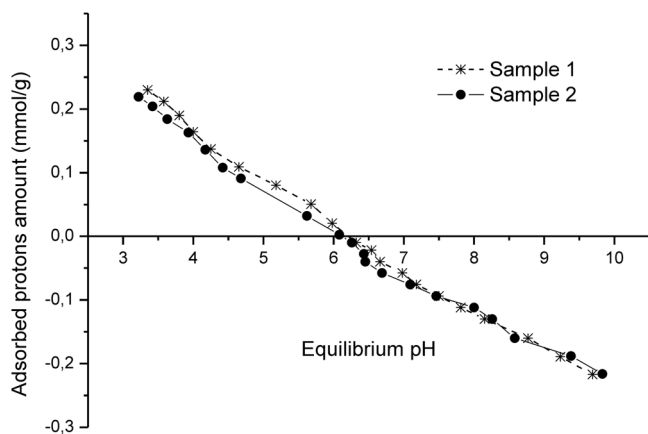


**Fig. 1.** Proton affinity curves of the  $\gamma$ -Al<sub>2</sub>O<sub>3</sub> support.

### 2.3. Catalytic tests

Catalytic tests for hydrogenation of toluene (Sigma Aldrich, 99%) were performed in a slurry Parr reactor at 373 K, under constant H<sub>2</sub> pressure of 5 MPa and at a stirring rate of 1000 rpm.

These tests were conducted with 25 mL of toluene, 30 mL of distilled water and 5 mL of *n*-heptane (Sigma Aldrich, 99%) used as internal standard for the chromatographic method. The presence of water is paramount in order to obtain partially hydrogenated products [12,37]. The *n*-heptane was considered to be a compound suitable for the analytical purposes, because it is very soluble in the organic phase (where the reaction products are) and easily separated from the reaction products during the chromatographic analysis, besides being chemically inert under the reaction conditions.

Samples of the organic phase were collected during the reaction and analyzed using an HP 5890 series II gas chromatograph equipped with a flame ionization detector and a 0.25 mm by 25 m capillary column of dimethylsiloxyane phase.

Conversion of toluene (X) and yield of methylcyclohexene (Y) were calculated according to Eqs. (1) and (2), respectively. The experimental values were used to adjust the Y versus X graph according to the reaction mass balance.

$$X = \frac{\text{moles of reacted toluene}}{\text{initial moles of toluene}} \quad (1)$$

$$Y = \frac{\text{moles of methylcyclohexene formed}}{\text{initial moles of toluene}} \quad (2)$$

In order to determine the initial reaction rate, instantaneous reaction rates were calculated from experimental data of toluene concentration versus reaction time. Through a linear fit of these rates, preferably for the values close to the beginning of the reaction, it was made an extrapolation to zero reaction time.

## 3. Results and Discussion

### 3.1. Proton affinity of the support and specific surface areas of solids

Since the  $\gamma$ -Al<sub>2</sub>O<sub>3</sub> support is known to exhibit an amphoteric behavior, the determination of its isoelectric point is essential for a better fixation of the metal cations by the wet impregnation method [38]. The Fig. 1 presents the proton affinity curves obtained for the  $\gamma$ -Al<sub>2</sub>O<sub>3</sub>, from which it was determined that the isoelectric point of this support is 6.2.

According to Kosmulski [39], the isoelectric point of  $\gamma$ -Al<sub>2</sub>O<sub>3</sub> is located between the pH of 7 and 8, while the value obtained in

**Table 1**  
Specific surface area ( $S_g$ ) and elementary chemical composition of solids.

Solid	$S_g$ (m <sup>2</sup> /g)	Mass fraction (%) by EDX				M/Ru atomic ratio nominal	by EDX	by XPS
		Al	O	Ru	M			
Al <sub>2</sub> O <sub>3</sub>	97.2	44	56	0.0	0.0	—	—	—
Pd/Al <sub>2</sub> O <sub>3</sub>	98.7	40	55	0.0	4.9	—	—	—
Pt/Al <sub>2</sub> O <sub>3</sub>	99.5	45	51	0.0	4.5	—	—	—
Ru/Al <sub>2</sub> O <sub>3</sub>	105	43	53	4.3	0.0	0.00	0.00	0.00
4Ru-1Pd/Al <sub>2</sub> O <sub>3</sub>	105	45	53	2.3	0.5	0.24	0.22	0.30
3Ru-2Pd/Al <sub>2</sub> O <sub>3</sub>	102	44	51	3.2	1.8	0.63	0.55	1.00
4Ru-1Pt/Al <sub>2</sub> O <sub>3</sub>	94.3	46	51	2.6	0.6	0.13	0.23	0.25
3Ru-2Pt/Al <sub>2</sub> O <sub>3</sub>	98.0	41	53	2.9	2.3	0.35	0.41	0.42
2Ru-3Pt/Al <sub>2</sub> O <sub>3</sub>	101	42	53	1.5	3.1	0.78	1.1	0.67

M: Pd or Pt.

the present study is slightly below this range. Such difference may be due to an inaccuracy of the potentiometric titration, since this technique is sensitive to the volume of electrolytes added during the procedure.

The pH of 10, much higher than the isoelectric point of the support, was adopted in this study for the wet impregnation in order to assure an efficient fixation of the noble metals. Particularly, since the aqua regia treatment of Pd and Pt precursors possibly formed [PdCl<sub>4</sub>]<sup>2-</sup> and [PtCl<sub>6</sub>]<sup>2-</sup>, the use of high pH condition is recommended by other researchers [40–42], according to whom it favors the formation of hydroxide species of these metals which are then deposited on alumina.

Specific surface areas of the studied solids are presented in Table 1. The results indicate an increase of the specific surface area for almost all catalysts with respect to the support. As suggested by Kawi et al. [43], such increase may be related to the formation of metal hydroxides by the addition of NaOH during the wet impregnation procedure. The formation of such hydroxides was observed in a previous study of our research group [11].

### 3.2. Chemical composition

Elementary chemical composition of studied solids, obtained through EDX analysis, is presented in Table 1, where M stands for metals (Pd or Pt) other than Ru.

For monometallic catalysts the respective metal load is very close to each other and to the desired amount (5 wt%). In turn, for the bimetallic catalysts the metal loads diverged from the nominal values, especially for low content of added metal (1 wt%). Increasing the amount of the added metal (e.g. 3Ru-2Pd/Al<sub>2</sub>O<sub>3</sub>), the metal load measured by EDX becomes closer to nominal values. Such effect can be due to the competitive adsorption of the metals on the support surface, which favors the Ru for low concentration of added metal.

As seen on Table 1, the M/Ru atomic ratios obtained by EDX are near to the respective nominal values. These results indicate that, despite deviation on the absolute amounts, both metals were fixated on the support in the desired proportion.

Nevertheless, the 2Ru-3Pt/Al<sub>2</sub>O<sub>3</sub> catalyst presented a Pt/Ru atomic ratio much higher than expected. This result may indicate a competitive adsorption of the metals, in which Pt cations are favored over those of Ru. The XPS analysis also allowed the evaluation of the relative M/Ru amounts on the surface of the catalysts, indicating an accordance to the EDX results for most of the solids.

The M/Ru atomic ratio of the 3Ru-2Pd/Al<sub>2</sub>O<sub>3</sub> catalyst was much higher when obtained by XPS than by EDX, which indicate that Pd is closer to the catalyst surface than Ru. This close proximity may be due to the coverage of Ru species by those of Pd.

In contrast, the 2Ru-3Pt/Al<sub>2</sub>O<sub>3</sub> catalyst presented a lower M/Ru ratio by XPS, suggesting that Ru is closer to the catalyst surface

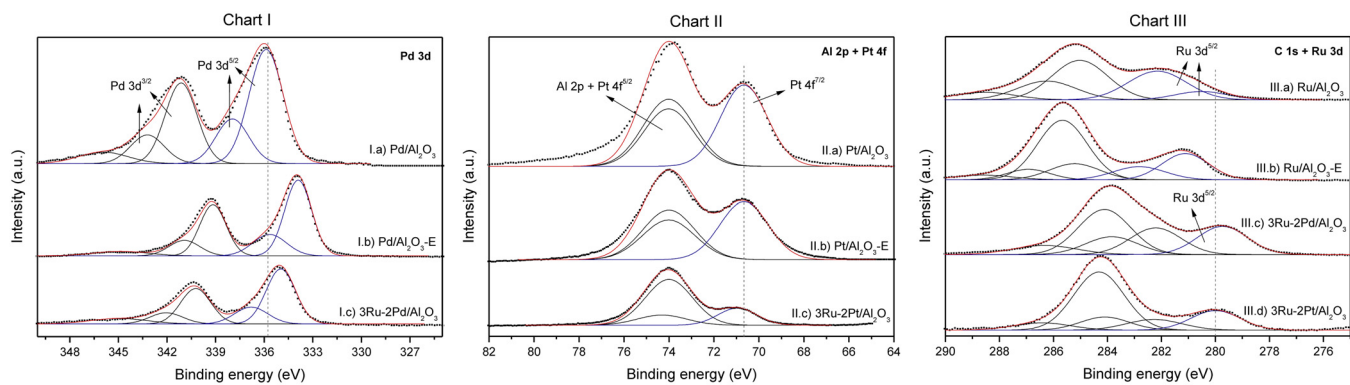


**Fig. 2.** Normalized XPS spectra of mono and bimetallic catalysts: Chart (I) Pd 3d, Chart II Al 2p + Pt 4f, Chart (III) C 1s + Ru 3d.

than Pt. Thus, this close proximity may be due to the coverage of Pt species by those of Ru.

No sodium or chlorine content was detected either by EDX or XPS in any prepared catalyst, which indicates an efficient removal of both ions by the washing of the solids.

XPS technique was also employed with the purpose of identifying the probable species of noble metals on the catalysts surfaces. The Fig. 2 presents the XPS spectra of Pd, Pt and Ru for selected mono and bimetallic catalysts. Binding energies of Pd 3d<sup>5/2</sup>, Pt 4f<sup>7/2</sup> and Ru 3d<sup>5/2</sup> for the analyzed solids are shown in Table 2.

The identification of the probable metal species was based on XPS patterns obtained from the National Institute of Standards and Technology (NIST)<sup>1</sup> and the La Surface<sup>2</sup> databases. No catalyst submitted to in situ activation was analyzed by XPS since other techniques indicated no significant effect on the formed species, as discussed hereafter.

In general, the XPS results show that the catalyst reduction in liquid phase led to the formation of metallic species, indicating that the reducing agent H<sub>2</sub>CO is able to reduce noble metal precursors in mild conditions. Nevertheless, the procedures for the catalyst activation have different influence on the formation of the metals species, notably depending on their nature.

Binding energies obtained for the non-activated Pd/Al<sub>2</sub>O<sub>3</sub> catalyst (335.8 and 338.0 eV) indicate the coexistence of the following phases: Pd<sup>0</sup> (335.3 eV) and PdO<sub>2</sub> (337.7 eV). In addition, the possible presence of Pd(OH)<sub>4</sub> (338.5 eV) suggests that H<sub>2</sub>CO could not reduce completely this compound to form Pd<sup>0</sup>, whereas the PdO<sub>2</sub> species may have been formed from oxidation of Pd<sup>0</sup> during the solid exposure to the atmospheric air.

Monometallic Pd catalyst activated ex situ (Pd/Al<sub>2</sub>O<sub>3</sub>-E) present a very low binding energy (334.0 eV) for Pd 3d<sup>5/2</sup>, not observed in the spectrum of non-activated Pd/Al<sub>2</sub>O<sub>3</sub> catalyst. Such low energy may be associated to the formation of aluminate phases like PdAl<sub>2</sub>O<sub>4</sub>, which may have been formed by interaction between Pd and Al<sub>2</sub>O<sub>3</sub> support. In addition, it has a binding energy of 335.7 eV corresponding to Pd<sup>0</sup> (335.3 eV) and possibly also to PdO (336.1 eV). The effect of the ex situ activation treatment for this solid may be observed in Fig. 2 (Chart I). For both solids (Fig. 2I.a and I.b) two distinct peaks are observed, however the ex situ activation led to a shift of these peaks towards lower binding energies for Pd 3d.

In turn, the binding energy of Pt 4f<sup>7/2</sup> for the non-activated Pt/Al<sub>2</sub>O<sub>3</sub> catalyst (70.7 eV) is probably related to Pt<sup>0</sup> (71.1 eV) as well as to a reducible form of Pt (PtO<sub>x</sub>-Al<sub>2</sub>O<sub>3</sub>), as suggested by the TPR results to be discussed posteriorly (Table 2). No binding

energies corresponding to phases PtO (73.6 eV) or Pt(OH)<sub>2</sub> (72.1 eV) were obtained (Fig. 2II.a).

In Fig. 2 (Chart II) one may observe that the ex situ activation treatment had little effect for Pt based catalysts. The ex situ activated Pt/Al<sub>2</sub>O<sub>3</sub>-E catalyst (Fig. 2II.b), presented the same binding energy of 70.7 eV as the non-activated solid, which seems to correspond to irreducible forms of Pt, as the TPR results indicate. It is noteworthy that only Pt 4f<sup>7/2</sup> binding energies were considered for this analysis, since the spectra of Pt 4f<sup>5/2</sup> overlap with the one of Al 2p (74 eV).

A non-reduced monometallic Ru catalyst (Ru/Al<sub>2</sub>O<sub>3</sub>-NR) was prepared with the purpose of being a baseline on the study about the role of the agent H<sub>2</sub>CO in the wet impregnation. The Ru 3d<sup>5/2</sup> binding energy of 281.6 eV may be related to the presence of Ru(OH)<sub>3</sub> formed by NaOH addition during the wet impregnation. The positive identification of Ru(OH)<sub>3</sub> via XPS is challenging and only recently Morgan [44] obtained an XPS pattern for this specie with Ru 3d<sup>5/2</sup> binding energy of 282.3 eV. Hence, since no chlorine from the RuCl<sub>3</sub> precursor was found on the Ru/Al<sub>2</sub>O<sub>3</sub>-NR solid either by EDX or XPS techniques, the formation of Ru hydroxides seems a plausible assumption.

Binding energies for non-activated Ru/Al<sub>2</sub>O<sub>3</sub> catalyst (280.5 and 282.1 eV) indicate the coexistence of Ru<sup>0</sup> (280.0 eV) and RuO<sub>3</sub> (282.3 eV), which may have been formed from Ru<sup>0</sup> phase during the exposure of the solid to the atmospheric air. However, the presence of Ru hydroxides cannot be discounted in this case, given the results of Morgan [44]. Nevertheless, these results indicate that similarly to the case of the Pd/Al<sub>2</sub>O<sub>3</sub> and Pt/Al<sub>2</sub>O<sub>3</sub> catalysts, Ru hydroxides can be reduced by H<sub>2</sub>CO in mild conditions.

The Fig. 2 (Chart III) shows that with the ex situ activation both Ru 3d<sup>5/2</sup> peaks are shifted towards higher binding energies (Fig. 2III.a and III.b). Indeed, XPS binding energies for the ex situ activated Ru/Al<sub>2</sub>O<sub>3</sub>-E catalyst (281.1 and 282.8 eV) are possibly related to oxides species RuO<sub>2</sub> (280.7 eV) and RuO<sub>3</sub> (282.3 eV). Along with the absence of Ru<sup>0</sup>, it seems that the ex situ activation induce an intense Ru oxidation when the catalyst is exposed to the contact with atmospheric air.

Given the XPS results obtained for monometallic catalysts, only the bimetallic solids reduced by H<sub>2</sub>CO and non-activated were characterized by XPS, in order to evidence the effect of the metal (Pd or Pt) loading to the bimetallic catalysts.

On both Ru-Pd catalysts (4Ru-1Pd/Al<sub>2</sub>O<sub>3</sub> and 3Ru-2Pd/Al<sub>2</sub>O<sub>3</sub>) the binding energies of Ru were considerably close (280.0 and 279.7 eV, respectively) and possibly related to the existence of Ru<sup>0</sup> species (280.0 eV). Whilst Ru remain on its reduced phase, the binding energies obtained for Pd on these solids (337.5 and 336.8 eV, respectively) suggest the existence of oxidized species such as PdO<sub>2</sub> (337.7 eV) and PdO (336.1 eV). Metallic Pd was also identified (335.0 eV), notably on the 3Ru-2Pd/Al<sub>2</sub>O<sub>3</sub> solid. Moreover, there is

<sup>1</sup> Data available at: <http://srdata.nist.gov/XPS>.

<sup>2</sup> Data available at: <http://lasurface.com/database/elementxps.php>.

**Table 2**

Physical and chemical characteristics of the catalysts.

Catalyst	TEM analysis		XPS analysis		Probable surface species <sup>a</sup>	TPR analysis		
			Binding energies (eV)			Temperature (K)	H <sub>2</sub> consumption (μmol <sub>H2</sub> /mg <sub>metal</sub> )	
	d <sub>p</sub> (nm)	σ (nm)	Metal (Pd 3d <sup>5/2</sup> or Pt 4f <sup>7/2</sup> )	Ru 3d <sup>5/2</sup>				
Pd/Al <sub>2</sub> O <sub>3</sub>	6.1	1.9	335.8; 338.0	—	Pd <sup>0</sup> ; PdO <sub>2</sub> ; Pd(OH) <sub>4</sub>	343	4.2	
Pd/Al <sub>2</sub> O <sub>3</sub> -E	29	13	334.0; 335.7	—	Pd-Al-O; Pd <sup>0</sup> ; PdO	339	6.7	
Pd/Al <sub>2</sub> O <sub>3</sub> -I	10	2.0	n.a.	—	n.a.	343	5.7	
Pt/Al <sub>2</sub> O <sub>3</sub>	3.3	0.72	70.7	—	Pt <sup>0</sup> ; PtO <sub>x</sub> -Al; Pt-Al-O	437	3.0	
						648	3.5	
Pt/Al <sub>2</sub> O <sub>3</sub> -E	n.a.	n.a.	70.7	—	Pt <sup>0</sup> ; Pt-Al-O	648	0.70	
Pt/Al <sub>2</sub> O <sub>3</sub> -I	n.a.	n.a.	n.a.	—	n.a.	351	0.30	
						648	5.0	
Ru/Al <sub>2</sub> O <sub>3</sub> -NR	n.a.	n.a.	—	281.6	Ru(OH) <sub>3</sub>	347	13	
Ru/Al <sub>2</sub> O <sub>3</sub>	6.2	0.75	—	280.5; 282.1	Ru <sup>0</sup> ; RuO <sub>3</sub>	353	3.4	
Ru/Al <sub>2</sub> O <sub>3</sub> -E	n.a.	n.a.	—	281.1; 282.8	RuO <sub>2</sub> ; RuO <sub>3</sub>	340	4.0	
						524	13	
Ru/Al <sub>2</sub> O <sub>3</sub> -I	n.a.	n.a.	n.a.	—	n.a.	333	7.0	
4Ru-1Pd/Al <sub>2</sub> O <sub>3</sub>	n.a.	n.a.	334.2; 337.5	280	Ru <sup>0</sup> ; Pd <sup>0</sup> ; PdO <sub>2</sub>	340	4.3	
4Ru-1Pd/Al <sub>2</sub> O <sub>3</sub> -E	n.a.	n.a.	n.a.	—	n.a.	333	2.6	
3Ru-2Pd/Al <sub>2</sub> O <sub>3</sub>	2.1	0.33	335.0; 336.8	279.7	Ru <sup>0</sup> ; Pd <sup>0</sup> ; PdO	328	4.0	
4Ru-1Pt/Al <sub>2</sub> O <sub>3</sub>	5.3	1.5	71.2	280	Ru <sup>0</sup> ; Pt <sup>0</sup>	358	4.6	
4Ru-1Pt/Al <sub>2</sub> O <sub>3</sub> -E	n.a.	n.a.	n.a.	—	n.a.	352	4.8	
3Ru-2Pt/Al <sub>2</sub> O <sub>3</sub>	1.6	0.43	71.0	280	Ru <sup>0</sup> ; RuO <sub>2</sub> ; Pt <sup>0</sup>	329	0.20	
						357	1.3	
2Ru-3Pt/Al <sub>2</sub> O <sub>3</sub>	2.8	0.85	70.8	279.2; 281.0	Ru <sup>0</sup> ; RuO <sub>2</sub> ; Pt <sup>0</sup>	356	2.9	
						533	2.0	

n.a.: solid not analyzed; d<sub>p</sub>: mean metallic particle diameter; σ: standard deviation of particle diameter.<sup>a</sup> binding energies patterns available at <http://lasurface.com/database/elementxps.php> and <http://srdata.nist.gov/XPS>.

no evidence of Pd(OH)<sub>4</sub> for Ru-Pd/Al<sub>2</sub>O<sub>3</sub> catalysts, in contrast to the monometallic Pd/Al<sub>2</sub>O<sub>3</sub> solid.

The XPS spectra for Pd and Ru obtained for the 3Ru-2Pd/Al<sub>2</sub>O<sub>3</sub> catalyst are presented in Fig. 2 (I.c and III.c spectra, respectively). Comparing the bimetallic with the monometallic spectra one may observe that both Ru and Pd are probably more reduced on the Ru-Pd/Al<sub>2</sub>O<sub>3</sub> solid. These results may be interpreted as a synergistic interaction between the metals in the sense that Ru seems to promote the reduction of Pd, whereas Pd inhibits the oxidation of Ru.

In turn, the XPS analyses of 3Ru-2Pt/Al<sub>2</sub>O<sub>3</sub> catalysts suggest that the addition of Pt also inhibits the oxidation of Ru (Fig. 2II.d and III.d, respectively). However this effect may be related to the amount of Pt added to the solid. Both catalysts with lower Pt amount (4Ru-1Pt/Al<sub>2</sub>O<sub>3</sub> and 3Ru-2Pt/Al<sub>2</sub>O<sub>3</sub>) presented Ru binding energies of 280.0 eV, evidencing that on these solids Ru is in its metallic phase. In contrast, for the 2Ru-3Pt/Al<sub>2</sub>O<sub>3</sub> catalyst, a second binding energy for Ru is observed (281.0 eV), which may be related to a RuO<sub>2</sub> species (280.7 eV). It is noteworthy that, similarly to monometallic catalysts, only Pt<sup>0</sup> binding energies were obtained on bimetallic Ru-Pt solids.

### 3.3. Metallic particle size

TEM technique was employed in order to investigate the effect of activation treatments on the size of metallic particles. Mean metallic particle diameters as well as their standard deviation are shown in Table 2.

As seen in Fig. 3 and Table 2, Pd particles with mean diameter of 6.1 nm are on the surface of the non-activated Pd/Al<sub>2</sub>O<sub>3</sub> catalyst (Fig. 3b), for which the standard deviation of particles diameter (1.9 nm) is relatively low, indicating a narrow size distribution.

The particle size of Pd increased substantially after in situ activation ( $10 \pm 2.0$  nm) and even more significantly for the ex situ activation ( $29 \pm 13$  nm), as seen on Fig. 3d and c, respectively. The Pd/Al<sub>2</sub>O<sub>3</sub>-E solid also presents a broader particle size distribution. These results suggest the occurrence of Pd sintering, due to high

activation temperatures respectively of 523 K and 573 K for in situ and ex situ activations.

According to Toebe et al. [30], even though Pd sintering temperature is elevated (ca. 1,050 K), this metal may experience mobility at temperatures as low as 423 K, mainly when exposed to H<sub>2</sub>.

Therefore, TEM results indicate that the activation of Pd catalysts under H<sub>2</sub> leads to a strong decrease of the metallic dispersion, which can consequently cause a decrease of the catalytic activity as presented hereafter. On the other hand, non-activated Pd/Al<sub>2</sub>O<sub>3</sub> catalyst reduced by H<sub>2</sub>CO in liquid phase under mild conditions, leads to small metal particles and high dispersion, as observed by Groppe et al. [28].

Non-activated Pt/Al<sub>2</sub>O<sub>3</sub> catalyst presents the smallest particles amongst the studied monometallic solids along with a very narrow size distribution ( $3.3 \pm 0.72$  nm). In turn, results in Table 2 show that non-activated Ru/Al<sub>2</sub>O<sub>3</sub> catalyst presents a mean metallic particle diameter of 6.2 nm, which is very close to that for non-activated Pd/Al<sub>2</sub>O<sub>3</sub> solid (6.1 nm), although Ru size distribution is much narrower (standard deviation of 0.75 nm).

Hence, the combined results of XPS and TEM suggest that the wet impregnation with reduction by H<sub>2</sub>CO is an efficient method to obtain well reduced catalysts with elevated metallic dispersion and narrow particle size distribution, notably for Ru and Pt. According to Irmak et al. [23], formaldehyde is a strong reducing agent, thus rapid nucleation could be realized by a fast reduction rate, which could explain the smaller metallic particles observed when this reducing agent is employed.

TEM results for non-activated bimetallic solids show that the addition of Pd or Pt to Ru/Al<sub>2</sub>O<sub>3</sub> catalysts decreases the mean metallic particle diameter and improves size uniformity (Fig. 4). In the case of Pd addition (Fig. 4b), the mean metallic particle diameter of 3Ru-2Pd/Al<sub>2</sub>O<sub>3</sub> catalyst ( $2.1 \pm 0.33$  nm) is smaller than the one obtained for both monometallic Pd/Al<sub>2</sub>O<sub>3</sub> (6.1 nm) and Ru/Al<sub>2</sub>O<sub>3</sub> (6.2 nm) solids (Figs. 3 b and 4 a, respectively). This effect was also observed by Romanenko et al. [31] for bimetallic Pd-Ru/C catalysts, which were considered to be more resistant to sintering than monometallic solids. Similar effects were also observed by

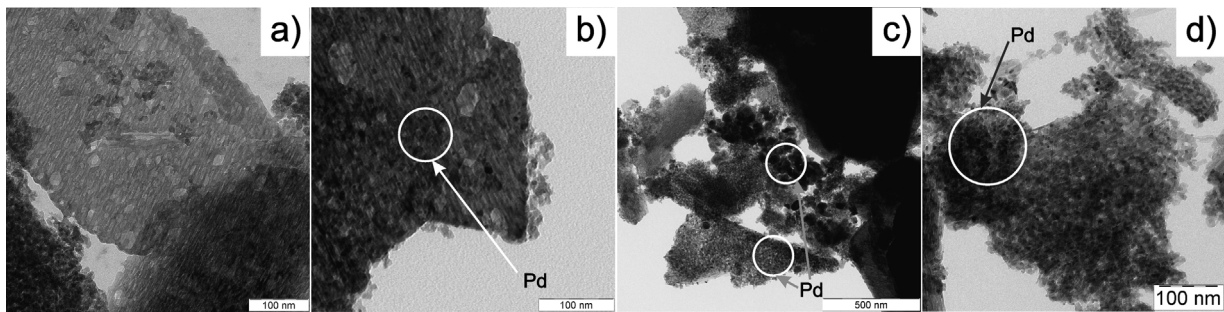


**Fig. 3.** TEM images: effect of the activation treatment on the morphology of the catalysts (a)  $\gamma\text{-Al}_2\text{O}_3$ , (b) Pd/ $\text{Al}_2\text{O}_3$ , (c) Pd/ $\text{Al}_2\text{O}_3$ -E and (d) Pd/ $\text{Al}_2\text{O}_3$ -I.

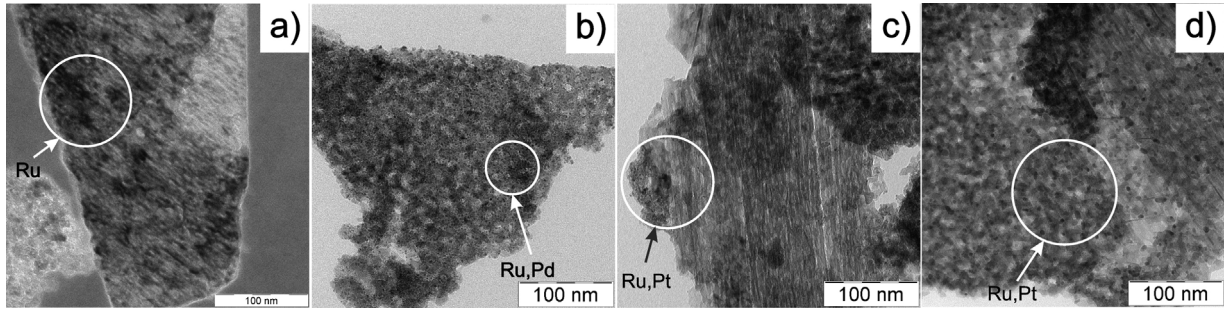


**Fig. 4.** TEM images: effect of noble metal (Pd, Pt) addition on the morphology of the catalysts (a) Ru/ $\text{Al}_2\text{O}_3$ , (b) 3Ru-2Pd/ $\text{Al}_2\text{O}_3$ , (c) 4Ru-1Pt/ $\text{Al}_2\text{O}_3$  and (d) 3Ru-2Pt/ $\text{Al}_2\text{O}_3$ .

Chen et al. [35], according to whom there is a contribution of Pd toward morphological features including the smaller nanoparticle size, narrower distribution and prevented particle aggregation.

Similarly to the bimetallic Pd-Ru system, the addition of Pt to Ru/ $\text{Al}_2\text{O}_3$  catalyst leads to a decrease of the mean metallic particle diameter, which passes through a minimum value ( $1.6 \pm 0.43$  nm) for the 3Ru-2Pt/ $\text{Al}_2\text{O}_3$  catalyst (Fig. 4d). The metallic particle sizes of Ru-Pt catalysts are close to what Liu et al. [34] obtained in their research (2–3 nm), also employing liquid-phase reduction procedures.

#### 3.4. Active phase formation

The temperatures of the  $\text{H}_2$  consumption peaks and the quantities of  $\text{H}_2$  consumption obtained from catalysts TPR profiles are presented in Table 2, whereas TPR profiles of non-activated mono and bimetallic catalysts are presented in Fig. 5.

Pd/ $\text{Al}_2\text{O}_3$  catalysts presented similar TPR profiles with a single  $\text{H}_2$  consumption peak at ca. 340 K (e.g. Fig. 5a), in which the corresponding  $\text{H}_2$  consumptions are very close to each other (ca.  $5.5 \pm 1.0 \mu\text{mol}$  of  $\text{H}_2/\text{mg}_{\text{Pd}}$ ). These  $\text{H}_2$  consumptions may be due to the reduction of Pd oxides and hydroxide.

Considering the stoichiometric values for the complete reduction of the  $\text{PdO}_2$  ( $19 \mu\text{mol}$  of  $\text{H}_2/\text{mg}_{\text{Pd}}$ ),  $\text{PdO}$  ( $9.4 \mu\text{mol}$  of  $\text{H}_2/\text{mg}_{\text{Pd}}$ ) and  $\text{Pd}(\text{OH})_4$  ( $19 \mu\text{mol}$  of  $\text{H}_2/\text{mg}_{\text{Pd}}$ ), the low  $\text{H}_2$  consumptions for Pd/ $\text{Al}_2\text{O}_3$  catalysts reinforces the presence of irreducible  $\text{Pd}^0$ , as suggested by XPS results.

TPR profile of non-activated Pt/ $\text{Al}_2\text{O}_3$  catalyst (Fig. 5b) show two  $\text{H}_2$  consumption peaks at 437 and 648 K. Authors [45–47] associated the existence of these peaks to the reduction of Pt species respectively in weak and strong interaction with the support.

Weak interaction may be associated with Pt oxides highly dispersed on the  $\text{Al}_2\text{O}_3$  support ( $\text{PtO}_x\text{-Al}$ ). In turn, aluminate species ( $\text{Pt-O-Al}$ ) would be in such a strong interaction with the support that would hardly be reducible, as suggested by XPS results and low  $\text{H}_2$  consumption ( $0.70 \mu\text{mol}$  of  $\text{H}_2/\text{mg}_{\text{Pt}}$ ) of the ex situ activated Pt/ $\text{Al}_2\text{O}_3$ -E catalyst.

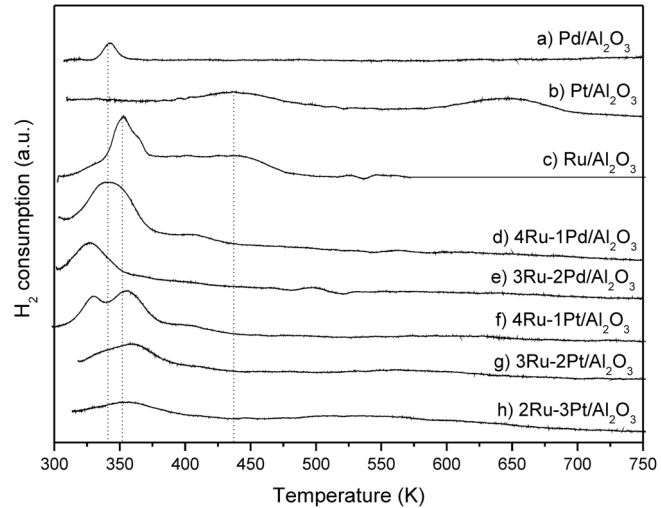


**Fig. 5.** TPR profiles of non-activated mono and bimetallic catalysts.

For non-reduced Ru/ $\text{Al}_2\text{O}_3$ -NR solid, the obtained  $\text{H}_2$  consumption ( $13 \mu\text{mol}$  of  $\text{H}_2/\text{mg}_{\text{Ru}}$ ) is very close to the stoichiometric value required for the complete reduction of the  $\text{Ru(OH)}_3$  ( $15 \mu\text{mol}$  of  $\text{H}_2/\text{mg}_{\text{Ru}}$ ). Such  $\text{H}_2$  consumption is much higher than that obtained for the reduced Ru/ $\text{Al}_2\text{O}_3$  catalyst ( $3.4 \mu\text{mol}$  of  $\text{H}_2/\text{mg}_{\text{Ru}}$ ). These results suggest that the agent  $\text{H}_2\text{CO}$  reduces the precursor  $\text{Ru(OH)}_3$  in liquid phase, which is consistent with the energies obtained by XPS.

The TPR profile of the Ru catalyst submitted to ex situ activation, Ru/ $\text{Al}_2\text{O}_3$ -E, presents two peaks of  $\text{H}_2$  consumption at low (340 K) and high (524 K) temperature. In this case, XPS results indicate a strong oxidation of the Ru with the coexistence of both  $\text{RuO}_2$  and  $\text{RuO}_3$  species, which is in agreement with the high overall  $\text{H}_2$  consumption obtained ( $17 \mu\text{mol}$  of  $\text{H}_2/\text{mg}_{\text{Ru}}$ ).

As observed for the Pd/ $\text{Al}_2\text{O}_3$  and Pt/ $\text{Al}_2\text{O}_3$  solids, TPR results for the Ru/ $\text{Al}_2\text{O}_3$  catalysts seem to indicate that the in situ acti-

vation has less effect than the ex situ activation on the active phase formation. TPR profile for the activated in situ catalyst, Ru/Al<sub>2</sub>O<sub>3</sub>-I, presents only one peak of H<sub>2</sub> consumption at low temperature (333 K), similar to the profile obtained for the non-activated Ru/Al<sub>2</sub>O<sub>3</sub> catalyst (Fig. 5c). However, the Ru/Al<sub>2</sub>O<sub>3</sub>-I catalyst presents a higher H<sub>2</sub> consumption, which suggests a stronger oxidation of the metal in comparison to the non-activated Ru/Al<sub>2</sub>O<sub>3</sub> catalyst.

TPR results for bimetallic Ru-Pd/Al<sub>2</sub>O<sub>3</sub> and Ru-Pt/Al<sub>2</sub>O<sub>3</sub> catalysts reinforces the possible existence of synergistic interactions between the metals, as reported by Romanenko et al. [31].

The addition of Pd to the non-activated Ru/Al<sub>2</sub>O<sub>3</sub> catalysts decreases the temperature of the single peak of H<sub>2</sub> consumption (Fig. 5d and e). This parameter (353 K for the monometallic Ru/Al<sub>2</sub>O<sub>3</sub>) decreases to 340 K (for the 4Ru-1Pd/Al<sub>2</sub>O<sub>3</sub> solid) and to 328 K (for the 3Ru-2Pd/Al<sub>2</sub>O<sub>3</sub> catalyst), thus being possibly related to the increase of the Pd content. In turn, the H<sub>2</sub> consumption slightly increases when Pd is present in the non-activated Ru/Al<sub>2</sub>O<sub>3</sub> catalyst.

Such results suggest that the presence of Pd promotes the catalyst reduction, which may be due to easier H<sub>2</sub> activation or higher dispersion of the metal. According to TEM results (Table 2), the size of metallic particle decreases for the bimetallic 3Ru-2Pd/Al<sub>2</sub>O<sub>3</sub> system with respect to their monometallic catalysts. This promotion effect was also observed by Chen et al. [35], whose results indicate that increasing the amount of Pd on the Ru based solid leads to lower reduction temperature peak and H<sub>2</sub> consumption.

The Pd presence in the ex situ activated Ru/Al<sub>2</sub>O<sub>3</sub>-E catalyst eliminates the peak of H<sub>2</sub> consumption at high temperature (524 K) and decrease intensely the H<sub>2</sub> consumption. Hence, the Pd addition seems to prevent the intense metal oxidation induced by ex situ activation.

Results show that the Pt addition to the Ru/Al<sub>2</sub>O<sub>3</sub> catalyst practically does not modify the temperature of the H<sub>2</sub> consumption peak (353 K) attributed to the reduction of RuO<sub>2</sub> phase (Fig. 5f–g).

On the other hand, the presence of Ru seems to promote the reduction of Pt species in the bimetallic catalysts, notably in the 3Ru-2Pt/Al<sub>2</sub>O<sub>3</sub> system, to which the H<sub>2</sub> consumption (1.5 μmol of H<sub>2</sub>/mg<sub>metal</sub>) is the lowest. These results indicate that most of the Ru and Pt in these solids are in metallic form, which is corroborated by the XPS analyses. Nevertheless, TPR profiles suggest the presence of small amounts of metal oxides in the Ru-Pt/Al<sub>2</sub>O<sub>3</sub> systems.

As observed in the case of Pd addition, the Pt presence in ex situ activated Ru/Al<sub>2</sub>O<sub>3</sub>-E catalyst eliminates the peak of H<sub>2</sub> consumption at high temperature (524 K) and decrease intensely the H<sub>2</sub> consumption. The association Ru-Pt also eliminates the peak of H<sub>2</sub> consumption at high temperature (623 K) observed on the TPR profile of the monometallic Pt/Al<sub>2</sub>O<sub>3</sub>-E system, attributed to species of the aluminate type.

### 3.5. Catalytic performance for toluene hydrogenation

Table 3 presents the catalytic performances of the studied solids for toluene hydrogenation in liquid phase. The reaction time of 360 min was chosen as pattern to compare the catalytic performances since it was sufficient time to reach total conversion of toluene for Ru based catalysts.

The obtained results show that the non-activated Pd/Al<sub>2</sub>O<sub>3</sub> and Pt/Al<sub>2</sub>O<sub>3</sub> catalysts present similar performances, while Ru/Al<sub>2</sub>O<sub>3</sub> solid is much more active and selective to methylcyclohexene.

Ru catalysts have been widely employed for aromatic hydrogenation reactions. Authors suggest that its remarkable activity and selectivity are due to the singular nature of this metal [11,17,18]. As reported by Kluson and Cerveny [17], toluene is more strongly adsorbed on Ru than on Pd surfaces. Such effect is associated to an

**Table 3**  
Catalytic performances for toluene hydrogenation in liquid phase.

Catalyst	<sup>a</sup> r <sub>0</sub>	X (%)	Y <sub>max</sub> (%)	X <sub>max</sub> (%)
Pd/Al <sub>2</sub> O <sub>3</sub>	5.3	7.0	0.0	–
Pd/Al <sub>2</sub> O <sub>3</sub> -E	1.7	2.4	0.0	–
Pd/Al <sub>2</sub> O <sub>3</sub> -I	2.0	3.6	0.15	2.2
Pt/Al <sub>2</sub> O <sub>3</sub>	5.3	7.0	1.0	7.0
Pt/Al <sub>2</sub> O <sub>3</sub> -E	2.7	4.2	0.16	2.7
Pt/Al <sub>2</sub> O <sub>3</sub> -I	1.3	1.5	0.13	1.1
Ru/Al <sub>2</sub> O <sub>3</sub> -NR	211	100	5.0	45
Ru/Al <sub>2</sub> O <sub>3</sub>	212	100	6.3	79
Ru/Al <sub>2</sub> O <sub>3</sub> -E	104	100	3.1	84
Ru/Al <sub>2</sub> O <sub>3</sub> -I	57	100	6.1	99
4Ru-1Pd/Al <sub>2</sub> O <sub>3</sub>	213	100	2.3	44
4Ru-1Pd/Al <sub>2</sub> O <sub>3</sub> -E	131	96	3.6	68
3Ru-2Pd/Al <sub>2</sub> O <sub>3</sub>	69	77	6.4	77
4Ru-1Pt/Al <sub>2</sub> O <sub>3</sub>	224	100	2.8	83
4Ru-1Pt/Al <sub>2</sub> O <sub>3</sub> -E	167	95	5.2	92
3Ru-2Pt/Al <sub>2</sub> O <sub>3</sub>	226	100	4.4	82
2Ru-3Pt/Al <sub>2</sub> O <sub>3</sub>	57	89	5.8	89

<sup>a</sup>r<sub>0</sub> in (mmol<sub>toluene</sub> L<sup>-1</sup> min<sup>-1</sup> g<sub>cat</sub><sup>-1</sup>): initial reaction rate.

X: conversion of toluene after 6 h of reaction.

Y<sub>max</sub>: maximum yield of methylcyclohexene.

X<sub>max</sub>: conversion of toluene at the maximum yield.

electron-deficient character of Ru, which could explain the higher activity observed in the present study regarding Ru/Al<sub>2</sub>O<sub>3</sub> catalysts.

As seen on Table 3, the non-reduced Ru/Al<sub>2</sub>O<sub>3</sub>-NR catalyst presents practically the same activity of the Ru/Al<sub>2</sub>O<sub>3</sub> solid reduced in liquid phase by H<sub>2</sub>CO. However, the reduced catalyst is more selective to methylcyclohexene at a higher conversion of toluene.

XPS and TPR results suggest the presence of Ru(OH)<sub>3</sub> on the surface of the non-reduced Ru/Al<sub>2</sub>O<sub>3</sub>-NR catalyst. Therefore, it seems reasonable to suppose that this hydroxide may be reduced in the reaction medium, where the reactant H<sub>2</sub> is present. The hydroxide reduction could lead to the Ru<sup>0</sup> formation and, consequently, to the coexistence of both metallic and cationic species, which is a necessary condition to the catalytic activity for aromatics hydrogenation [20,48].

#### 3.5.1. Effects of the catalyst activation

Results presented in Table 3 indicate that both ex situ and in situ activations decrease the initial activity of the studied mono and bimetallic catalysts.

As seen by TEM analysis, both ex situ and in situ activations increase the metallic particles size of Pd/Al<sub>2</sub>O<sub>3</sub> catalyst. Such decrease of the metal dispersion is possibly due to the occurrence of sintering, which is an effect of catalysts activation according to previous studies [28–30].

XPS and TPR characterizations of the Pt/Al<sub>2</sub>O<sub>3</sub>-E catalyst activated ex situ suggest a complete reduction of the Pt species and a strong metal-support interaction. In this case, the decrease in the catalytic activity induced by the ex situ activation may be related to a low amount of Pt<sup>0+</sup> sites.

Taimoor and Pitault [48] conducted a kinetic study about the gas phase hydrogenation of toluene on Pt catalysts. The authors propose that metallic sites as well cationic sites (metal-support interaction) have both an important role in this reaction. According to the authors, H<sub>2</sub> would be adsorbed on metallic sites, whereas toluene would be adsorbed on cationic sites.

The activity loss observed for activated Ru/Al<sub>2</sub>O<sub>3</sub>-E and Ru/Al<sub>2</sub>O<sub>3</sub>-I catalysts may be due to the probable formation of Ru oxides, as indicated by the XPS results. In turn, TPR analyses suggest that the reduction of such oxides may be more difficult and, consequently, the Ru<sup>0</sup>/Ru<sup>δ+</sup> ratio might be affected.

After 360 min of reaction, the conversion of toluene is practically total for the Ru based catalysts, due to their high activities, while it is less than 7% for the monometallic Pd/Al<sub>2</sub>O<sub>3</sub> and Pt/Al<sub>2</sub>O<sub>3</sub> solids.

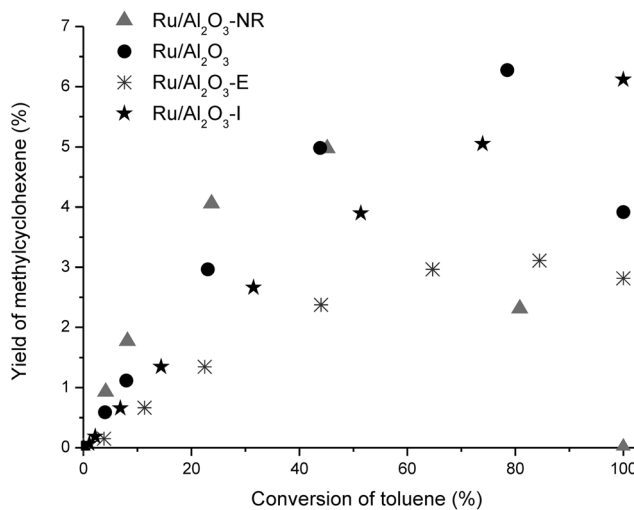


Fig. 6. Effect of the reduction method on the yield of methylcyclohexene for the Ru/Al<sub>2</sub>O<sub>3</sub> catalysts.

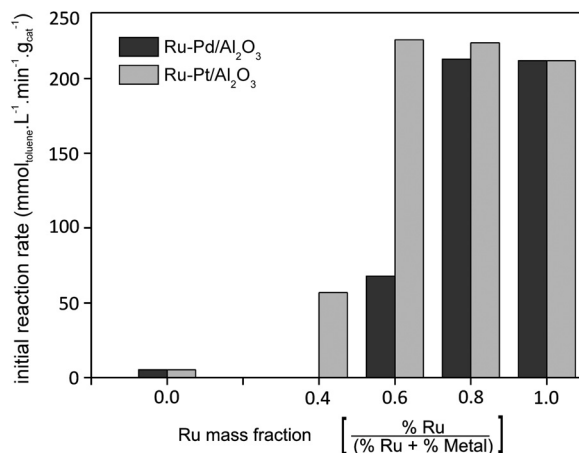


Fig. 7. Influence of Pd or Pt addition on the initial reaction rate of non-activated Ru/Al<sub>2</sub>O<sub>3</sub> based catalysts.

The Fig. 6 presents the evolution of the yield of methylcyclohexene during the reaction course (toluene conversion) for the monometallic Ru/Al<sub>2</sub>O<sub>3</sub> catalysts.

Although the non-reduced Ru/Al<sub>2</sub>O<sub>3</sub>-NR catalyst has an initial activity comparable to the Ru/Al<sub>2</sub>O<sub>3</sub> solid reduced by H<sub>2</sub>CO, the latter leads to higher yields of methylcyclohexene at high toluene conversion. As observed by Zhou et al. [49], non-reduced Ru catalysts treated with hydroxides display remarkable performance on the hydrogenation of aromatics. These authors attributed this result to base electronic promotion, blockade of cyclohexene chemisorption sites and OH<sup>-</sup> hydrophilic increment effect.

According to, Mazzieri et al. [20], Taimoor and Pitault [48] and Zanabaev et al. [50], a reasonable balance between Ru<sup>0</sup> and Ru<sup>δ+</sup> species is important for the formation of the intermediate product of hydrogenation.

### 3.5.2. Effects of the Pd and Pt load

Bimetallic Ru-Pd/Al<sub>2</sub>O<sub>3</sub> and Ru-Pt/Al<sub>2</sub>O<sub>3</sub> catalysts containing different amounts of noble metals were prepared in order to investigate the effects of the Pd or Pt addition on the performance of Ru/Al<sub>2</sub>O<sub>3</sub> based catalysts for hydrogenation of toluene. Results of the catalytic tests are given in Table 3, whereas in Fig. 7 the initial reaction rate for the studied catalysts are compared in regards to the Ru mass fraction of these solids.

The addition of Pd to the Ru/Al<sub>2</sub>O<sub>3</sub> catalyst leads to a decrease of the yield of methylcyclohexene, as observed for the 4Ru-1Pd/Al<sub>2</sub>O<sub>3</sub> system, although this does not change the initial reaction rate. Increasing the Pd load, the 3Ru-2Pd/Al<sub>2</sub>O<sub>3</sub> system presents a higher selectivity at the expense of a significant loss of catalytic activity, being unable to achieve total conversion within 360 min of reaction.

XPS results (Table 2) indicate the presence of PdO<sub>2</sub> and PdO respectively in 4Ru-1Pd/Al<sub>2</sub>O<sub>3</sub> and 3Ru-2Pd/Al<sub>2</sub>O<sub>3</sub> systems. These oxides could cover the particles of Ru, leading to a decrease in catalytic activity observed when the Pd content increases.

In turn, the addition of Pt to the Ru/Al<sub>2</sub>O<sub>3</sub> catalyst increases the initial reaction rate in the case of the 4Ru-1Pt/Al<sub>2</sub>O<sub>3</sub> and 3Ru-2Pt/Al<sub>2</sub>O<sub>3</sub> systems, at the expense of their selectivity, a result predicted by Liu et al. [34]. The initial activity decreases remarkably with increasing Pt load (2Ru-3Pt/Al<sub>2</sub>O<sub>3</sub> catalyst), similarly to that observed for the 3Ru-2Pd/Al<sub>2</sub>O<sub>3</sub> system.

TEM results (Table 2) indicate that the bimetallic Ru-Pt/Al<sub>2</sub>O<sub>3</sub> systems present smaller metallic particles (higher metal dispersion) than the monometallic Ru/Al<sub>2</sub>O<sub>3</sub> catalyst, which may be the cause of increased catalytic activity. As explained by Liu et al. [34], smaller metal particles can offer higher reactivity in catalysis, due to their higher surface to volume ratio and thus larger surface areas exposed to reactants.

XPS analysis shows the presence of RuO<sub>2</sub> in the 2Ru-3Pt/Al<sub>2</sub>O<sub>3</sub> catalyst (Table 2), which may have led to lower activity, as observed in the cases of the activated monometallic Ru/Al<sub>2</sub>O<sub>3</sub>-E and Ru/Al<sub>2</sub>O<sub>3</sub>-I catalysts.

Such results indicate the existence of a synergistic effect induced by the Pt addition on the catalytic activity of Ru/Al<sub>2</sub>O<sub>3</sub> based catalysts for toluene hydrogenation in liquid phase. Similar effects were observed by Liu et al. [34], according to whom the synergistic interaction between these metals may be related to the electronic modification in a bimetallic surface through the formation or core-shell morphologies.

## 4. Conclusions

Results of the present study show that the addition of noble metals Pd and Pt induce remarkable effects on the morphology and performance of Ru/Al<sub>2</sub>O<sub>3</sub> based catalysts for toluene hydrogenation in liquid phase.

Reduction by formaldehyde during catalysts preparation through wet impregnation leads to the formation of metallic species from chlorinated precursors. Subsequent ex situ or in situ activation under H<sub>2</sub> form Pd and Ru oxides and decrease the catalytic activity.

Initial reaction rates of non-activated catalysts follow the order: Ru/Al<sub>2</sub>O<sub>3</sub> ≫ Pd/Al<sub>2</sub>O<sub>3</sub> ≈ Pt/Al<sub>2</sub>O<sub>3</sub>. A synergistic effect on the catalytic activity can be induced by the Pt addition to Ru/Al<sub>2</sub>O<sub>3</sub> based catalysts.

## Acknowledgements

To the “National Counsel of Technological and Scientific Development” (CNPq) for the financial support and research scholarship granted to Raphael Soeiro Suppino.

## References

- [1] K. Sato, M. Aoki, R. Noyori, Science 281 (1998) 1646–1647.
- [2] E. Dietzsch, P. Claus, D. Hönicke, Top. Catal. 10 (2000) 99–106.
- [3] M. Zhou, G. Lin, H. Zhang, Chin. J. Catal. 28 (2007) 210–216.
- [4] T. Fujikawa, K. Idei, T. Ebihara, H. Mizuguchi, K. Usui, Appl. Catal. A Gen. 192 (2000) 253–261.
- [5] H. Backman, A.K. Neyestanaki, D.Y. Murzin, J. Catal. 233 (2005) 109–118.
- [6] L. Ronchin, L. Toniolo, Appl. Catal. A Gen. 208 (2001) 77–89.
- [7] J. Wang, Y. Wang, S. Xie, M. Qiao, H. Li, K. Fan, Appl. Catal. A Gen. 272 (2004) 29–36.

- [8] J. Bu, Y. Pei, P. Guo, M. Qiao, S. Yan, K. Fan, *Stud. Surf. Sci. Catal.* 165 (2007) 769–772.
- [9] P.d.C. Zonetti, R. Landers, A.J.G. Cobo, *Appl. Surf. Sci.* 254 (2008) 6849–6853.
- [10] C. Zanutelo, R. Landers, W.A. Carvalho, A.J.G. Cobo, *Appl. Catal. A Gen.* 409 (2011) 174–180.
- [11] R.S. Suppino, R. Landers, A.J.G. Cobo, *Appl. Catal. A Gen.* 452 (2013) 9–16.
- [12] L. Foppa, J. Dupont, *Chem. Soc. Rev.* 44 (2015) 1886–1897.
- [13] M. Saefs, M.-F. Reyniers, J.W. Thybaut, M. Neurock, G.B. Marin, *J. Catal.* 236 (2005) 129–138.
- [14] F. Alhumaidan, D. Cresswell, A. Garforth, *Energy Fuel* 25 (2011) 4217–4234.
- [15] J.N. Stanley, F. Heinroth, C.C. Weber, A.F. Masters, T. Maschmeyer, *Appl. Catal. A Gen.* 454 (2013) 46–52.
- [16] S. Hu, M. Xue, H. Chen, Y. Sun, J. Shen, *Chin. J. Catal.* 32 (2011) 917–925.
- [17] P. Kluson, L. Cerveny, *Appl. Catal. A Gen.* 128 (1995) 13–31.
- [18] P. Kluson, J. Had, Z. Belohlav, L. Cerveny, *Appl. Catal. A Gen.* 149 (1997) 331–339.
- [19] L. Zhu, H. Sun, H. Fu, J. Zheng, N. Zhang, Y. Li, B.H. Chen, *Appl. Catal. A Gen.* 499 (2015) 124–132.
- [20] V.A. Mazzieri, P.C. L'Argentiére, F. Coloma-Pascual, N.S. Figoli, *Ind. Eng. Chem. Res.* 42 (2003) 2269–2272.
- [21] J.-L. Liu, L.-J. Zhu, Y. Pei, J.-H. Zhuang, H. Li, H.-X. Li, M.-H. Qiao, K.-N. Fan, *Appl. Catal. A Gen.* 353 (2009) 282–287.
- [22] P. Mäki-Arvela, D.Y. Murzin, *Appl. Catal. A Gen.* 451 (2013) 251–281.
- [23] S. Irmak, B. Meryemoglu, B.K. Ozsel, A. Hasanoglu, O. Erbatur, *Int. J. Hydrogen Energy* 40 (2015) 14826–14832.
- [24] C. Roth, N. Martz, H. Fuess, *PCCP* 3 (2001) 315–319.
- [25] G.-Y. Fan, W.-D. Jiang, J.-B. Wang, R.-X. Li, H. Chen, X.-J. Li, *Catal. Commun.* 10 (2008) 98–102.
- [26] Á. Szegedi, M. Popova, V. Mavrodinova, C. Minchev, *Appl. Catal. A Gen.* 338 (2008) 44–51.
- [27] P.G. Savva, K. Goundani, J. Vakros, K. Bourikas, C. Fountzoula, D. Vattis, A. Lycourghiotis, C. Kordulis, *Appl. Catal. B Environ.* 79 (2008) 199–207.
- [28] E. Groppo, G. Agostini, A. Piovano, N.B. Muddada, G. Leofanti, R. Pellegrini, G. Portale, A. Longo, C. Lamberti, *J. Catal.* 287 (2012) 44–54.
- [29] R. Pattabiraman, *Appl. Catal. A Gen.* 153 (1997) 9–20.
- [30] M.L. Toebes, J.A. van Dillen, K.P. de Jong, *J. Mol. Catal. A: Chem.* 173 (2001) 75–98.
- [31] A. Romanenko, E. Tyschishin, E. Moroz, V. Likholobov, V. Zaikovskii, S. Jhung, Y.-S. Park, *Appl. Catal. A Gen.* 227 (2002) 117–123.
- [32] S. Loiha, K. Fötinger, K. Zorn, W. Klysubun, G. Rupprechter, J. Wittayakun, *J. Ind. Eng. Chem.* 15 (2009) 819–823.
- [33] Y. Yu, O.Y. Gutierrez, G.L. Haller, R. Colby, B. Kabius, J. Rob van Veen, A. Jentys, J.A. Lercher, *J. Catal.* 304 (2013) 135–148.
- [34] H. Liu, R. Fang, Z. Li, Y. Li, *Chem. Eng. Sci.* 122 (2015) 350–359.
- [35] J. Chen, X. Liu, F. Zhang, *Chem. Eng. J.* 259 (2015) 43–52.
- [36] V. Strelko, D.J. Malik, *J. Colloid Interface Sci.* 250 (2002) 213–220.
- [37] M.M. Johnson, G.P. Nowack, *J. Catal.* 38 (1975) 518–521.
- [38] J.P. Brunelle, *Stud. Surf. Sci. Catal.* 3 (1979) 211–232.
- [39] M. Kosmulski, *Surface Charging and Points of Zero Charge*, CRC Press, Boca Raton, Florida, United States of America, 2009.
- [40] K. Köhler, R.G. Heidenreich, S.S. Soomro, S.S. Pröckl, *Adv. Synth. Catal.* 350 (2008) 2930–2936.
- [41] O.A. Simakova, P.A. Simonov, A.V. Romanenko, I.L. Simakova, *React. Kinet. Catal. Lett.* 95 (2008) 3–12.
- [42] O. Belskaya, V. Duplyakin, V. Likholobov, *Smart Nanocomposites* 1 (2011) 99–133.
- [43] S. Kawi, S.Y. Liu, S.C. Shen, *Catal. Today* 68 (2001) 237–244.
- [44] D.J. Morgan, *Surf. Interface Anal.* 47 (2015) 1072–1079.
- [45] O.A. Bariás, A. Holmen, E.A. Blekkan, *J. Catal.* 158 (1996) 1–12.
- [46] S. De Miguel, M. Román-Martínez, D. Cazorla-Amorós, E. Jablonski, O. Scelza, *Catal. Today* 66 (2001) 289–295.
- [47] P.T. Do, M. Chiappero, L.L. Lobban, D.E. Resasco, *Catal. Lett.* 130 (2009) 9–18.
- [48] A.A. Taimoor, I. Pitault, *React. Kinet. Mech. Catal.* 102 (2011) 263–282.
- [49] G. Zhou, X. Tan, Y. Pei, K. Fan, M. Qiao, B. Sun, B. Zong, *Chem. Cat. Chem.* 5 (2013) 2425–2435.
- [50] B. Zhanabaev, P. Zanozina, B. Utelbaev, *Kinet. Catal.* 32 (1991) 191–194.